Two-Dimensional Simulation on Detonation Wave Supported by the Cylindrical Inner Wall Injecting Premixed Gas

Junpei FUJII[1], Akiko MATSUO[1], Jiro KASAHARA[2]

[1]Department of Mechanical Engineering, Keio University, Yokohama, Kanagawa, Japan

[2]Department of Aerospace Engineering, Nagoya University, Nagoya, Aichi, Japan

1 Introduction

Detonation is one of the premixed combustion modes propagating with a shock wave. Detonation gives some merits to internal combustion engines of supersonic transports. For instance, it can improve their thermal efficiencies. It can also simplify their structures because mechanical compressors are not needed. In the current studies, Pulse Detonation Engine (PDE) is widely known as one of the internal combustion engines using detonation. PDE obtains a intermittent thrust by repeating a cycle; the chamber is filled with premixed gas, the detonation wave is made by an igniter and burned gas is released. PDE has to deal with the problem that it needs to achieve a stable thrust with its intermittent behavior. Rotating Detonation Engine (RDE) is also known as the engine using detonation. RDE obtains a stable thrust by detonation waves. The thermal efficiency and the specific impulse of RDE are equal to those of PDE, and RDE has merits that a detonation wave exists continuously once starting an engine. There are also some problems for RDE for a practical use. The efficient cooling system is needed for RDE to run for a long time due to the existence of a detonation wave which has high temperatures and high pressures [1]. Various experiments and numerical simulations aiming for the stable operation of RDE have been carried out. Numerical approaches have the advantage of tracing the behavior of the detonation wave propagating supersonically within the chamber. Kailasanath et al. [2] investigated the effect of injection nozzles and chamber scale for the flow field in RDE chamber. The researches on RDE have mainly aimed for the annular ring combustion chamber. Here, the optimum design of RDE chamber is not clear. Vasil'ev [3] tried to explore the physical mechanism of detonation wave along the gaseous layer around the cylinder in an experimental way, and further study is still needed for the knowledge of flow field within RDE.

This study focuses on the behavior of two-dimensional detonation wave supported by the cylindrical inner wall injecting premixed gas. First, a longitudinal chamber length is taken as a parameter in the rectangular flow field, which is related to the method of two-dimensional RDE simulations to get the reference data for comparison. Secondly, a radius of curvature is taken as a parameter, where the arc-shaped flow field is used instead of the whole area around the cylinder. Thirdly, a length of inner arc, which corresponds to the number of detonation around the cylinder, is

Correspondence to: tktsk.jwingsf.10okfor.br_f.65@keio.jp

taken as a parameter in the arc-shaped flow field. The aim of this study is to clarify the condition to propagate a detonation wave consuming the injecting premixed gas from the cylindrical inner wall.

2 Numerical setup

The governing equations are the two-dimensional compressive Euler Equations. Chemical model is a two-step reaction model proposed by Korobeinikov et al [4]. The convection term is discretized by Yee's Non-MUSCL Type 2nd-Order Upwind Scheme. Point-Implicit Method that only treats source term implicitly is adopted as the time integration. Stoichiometric Hydrogen-Air mixtures are the target fluid of this study.

Figure 1 shows the computational grids and boundary conditions of this study. The domains are corresponding to (a) the rectangular flow field whose longitudinal chamber length, L, is taken as a parameter, and (b) the arc-shaped flow field whose radius of curvature, r_{in}, is taken as a parameter. θ is also defined as the parameter corresponding to r_{in}. The minimum grid size is 40 μm for both domains. The domains are composed of non-stretch and stretch regions. In the initial state of the flow field, one-dimensional steady detonation wave is set from the origin to ξ = 8 mm for the whole η direction. The premixed unburned mixture at p = 1 atm and T = 293 K filled the area in front of the detonation wave. Left and right ends of the domain are treated as periodic boundaries. At the upper end, outflow boundary condition depending on the Mach number is adopted. At the lower end, converging injection nozzles whose width is 40 μm, are set at 200 μm intervals. Their total pressure of p_0 = 10 atm and total temperature of T_0 = 293 K are defined as constant. The boundary condition at the lower end is defined by the relation between p_0 and the pressure one point from the lower end, which depends on the location of the detonation wave. Adiabatic rigid wall is adopted for the lower end without nozzle.

First, L = 50, 60, 75 and 100 mm are used to investigate the effect of longitudinal chamber length in the rectangular flow field. Secondly, r_{in} = 191, 127, 95.5, 79.6 and 63.7 mm (θ = 30˚, 45˚, 60˚, 72˚ and 90˚) at constant L = 100 mm are used to investigate the effect of the curvature in the arc-shaped flow field. Thirdly, L = 75, 100, 150 and 200 mm (θ = 45˚, 60˚, 90˚ and 120˚) at constant r_{in} = 95.5 mm are also investigated in the arc-shaped flow field.

In this study, cycle number, *#c*, is introduced to indicate the location of the detonation wave propagating in the chamber with the periodic boundary condition. The value of *#c* is derived from the position of detonation wave one point above the lower end, and starts at *#c* = 1.00. The non-stretch region height at their domains is set as the following conditions: 14 mm to all cases in the rectangular flow field, r_{in} = 191 and 127 mm at L = 100 mm and r_{in} = 95.5 mm at L = 75 mm in the arc-shaped flow field. 28 mm to r_{in} = 95.5, 79.6 and 63.7 mm at L = 100 mm and r_{in} = 95.5 mm at L = 150 mm in the arc-shaped flow field. 40 mm to L = 200 mm at constant r_{in} = 95.5 mm in the arc-shaped flow field. The height dependency is validated with four cases of 8, 14, 28 and 40 mm in the rectangular flow field at L = 100 mm. Here, h is newly defined as the distance from the lower end to the maximum point of unburned mixtures. Figure 2 shows *#c* history of the detonation height, h, and their values of h converge to a constant value. Their way of convergence is also quantitatively similar. Consequently, the non-stretch region height of each domain is set to be adequate to trace the highest point of the detonation front.

3 Results and Discussions

3.1 Rectangular flow field

The detonation wave kept propagating in L = 60, 75 and 100 mm, and it collapsed in L = 50 mm at *#c* = 3.79. Figure 3 shows the typical steady flow field of temperature using the data in L = 100 mm at *#c* = 8.50. There is the zone with no injection behind the detonation wave above the bottom wall in the figure. It indicates that the pressure is higher than p_0, and the same phenomena appeared in L = 60 and 75 mm. Figure 4 shows *#c* histories of (a) the injection rate, defined by the relation between the summation of the local mass flow rate and the total mass flow rate at all nozzle choked, and (b) the propagation velocity. The injection rate of L = 60, 75 and 100 mm converge to the same value of

81.0%. The propagation velocity of L = 60, 75 and 100 mm also converge to the same value of 1875 m/s, which is 97.0% of the CJ velocity. Here, the CJ velocity of 1930 m/s is derived from the flow variables in front of the detonation wave. Table 1 shows the values of h at steady state, h_{steady}, the propagation velocity, D_{steady}, and h_{steady}/L in the cases of L = 60, 75 and 100 mm. It indicates that there is a similarity in h_{steady}/L as 0.112. Figure 5 shows #c history of h in all case. It can be confirmed that the timing of convergence is different from each other in stable cases, and it gets earlier as L increases.

3.2 Arc-shaped flow field

In this study, the arc-shaped flow field is utilized instead of the whole flow field around the cylindrical inner wall injecting premixed gas, and it corresponds to a part of the flow field where the successive flow pattern appears around cylinder. Here, the above assumption is validated using the following. The steady flow field is achieved in the arc-shaped computational domain in the case of r_{in} = 95.5 mm (θ = 60˚) and L = 100 mm, and the simulated data is successively put around the cylinder. After that, the simulation around the cylinder is started. Figure 6 shows (a) the steady flow field in the case of r_{in} = 95.5 mm and L = 100 mm at #c = 9.83, and (b) the flow field around cylinder at 200 μs after the restart. The simulation around the cylinder settled down to the steady propagation, and the characteristics are the same as those in the arc-shaped flow field. It indicates that the simulation result of the arc-shaped flow field represents that around the cylinder.

3.3 The effect of the radius of curvature at constant L = 100 mm

The detonation wave kept propagating in r_{in} = 191, 127 and 95.5 mm, and it collapsed in r_{in} = 79.6 mm at #c = 5.63 and r_{in} = 63.7 mm at #c = 5.31. Figure 7 shows the typical steady flow field of temperature in r_{in} = 191 mm (θ = 30˚) at #c = 8.50. The flow characteristics are similar to those of Figure 3, as well as the cases of r_{in} = 127 and 95.5 mm. Figure 8 shows #c histories of (a) the injection rate and (b) the propagation velocity in stable cases, and the black lines are the results of the rectangular case. In the injection rate of Figure 8 (a), the values of convergence in r_{in} = 191, 127 and 95.5 mm are 84.2, 85.6 and 86.7%, respectively, and they are slightly larger than that of the rectangular case of 81.0%. The increase of the values is also started at about #c = 5.00, and the timing is earlier as r_{in} decreases. In the propagation velocity of Figure 8 (b), the values of convergence in r_{in} = 191, 127 and 95.5 mm are 1850, 1840 and 1830 m/s, respectively, and they are smaller than that of the rectangular case of 1875 m/s. Here, the CJ velocity is 1930 m/s. Figure 9 shows #c history of h, which is divided into three phases; firstly the dominance of the initial disturbance at #c = 2.00 – 4.00, secondly the increase at #c = 4.00 – 6.00 and thirdly the convergence after #c = 6.00.

Table 2 shows the values of h_{steady} and D_{steady}. Since the detonation wave in the cases of r_{in} = 79.6 and 63.7 mm collapsed, $h_{collapsed}$ is derived from #c = 5.63 and #c = 5.31. The values of h_{steady}/L are slightly larger than those of the rectangular case. This tendency also gets stronger as r_{in} decreases. Here, L_h is newly introduced as the length of inner wall at $r_{in} + h_{steady}$. In the steady cases of r_{in} = 191, 127 and 95.5 mm, their values of h_{steady}/L_h are about 0.117 and are close to the h_{steady}/L of rectangular cases. D_h is also newly introduced as the propagation velocity at the highest point of the detonation front, and $D_{h/2}$ is derived from the average of D_{steady} and D_h. The velocities at D_h are more than the CJ velocity, and those at $D_{h/2}$ are very close to the CJ velocity. Therefore, the case of r_{in} = 95.5 mm would be a critical condition, and the smaller r_{in} cases could not achieve steady propagation.

3.4 The effect of the length of inner arc at constant r_{in} = 95.5 mm

The detonation wave kept propagating in all cases, and Figure 10 shows #c histories of (a) the injection rate and (b) the propagation velocity. In the injection rate of Figure 10 (a), the value of convergence is slightly larger and the increase of the values is also started earlier as L increases. On the other hand, the propagation velocity in each case converges the same value of 1830 m/s, which are 94.8% of the CJ velocity (1930 m/s) though the vibration due to the initial disturbance appears. Figure 11 indicates #c histories of h, which is also divided into three phases as well as Figure 9. Table 3 shows the values of h_{steady} and D_{steady}. The values of h_{steady} get larger as L increases, and the values of h_{steady}/L_h are close to those of Tables 1 and 2. The values of D_h are much higher than the CJ velocity

due to the effect of curvature, although the propagation velocity near the wall is lower than it. In the case of L = 200 mm, more than 80% of the detonation front is over CJ velocity, but the detonation wave did not collapse. Therefore, the critical condition of steady propagation would be different from that in the section 3.3.

4 Conclusion

Propagation of detonation wave supported by the cylindrical inner wall injecting premixed hydrogen-air gas mixture was numerically investigated. The propagation depended not only on the mass flow rate and the propagation velocity, but also on the detonation height. In the rectangular domain, flow field of L = 60, 75 and 100 mm got stable, but that of the smaller length case of L = 50 mm could not show the steady propagation. In the arc-shaped domain at constant L = 100 mm, the case of r_{in} = 95.5 mm would be a critical condition, and the smaller r_{in} cases could not achieve steady propagation. In the arc-shaped domain at constant r_{in} = 95.5 mm, the collapse of detonation wave was not confirmed, and the critical condition would be different from the cases of constant L = 100 mm.

References

[1] Tsuboi N et al. (2013). Rotating Detonation Engines. J. Combustion and Society of Japan, 55:174.

[2] Kailasanath K et al. (2014). Towards Efficient, Unsteady, Three-Dimensional Rotating Detonation Engine Simulations. AIAA Paper 2014-1014.

[3] A. A. Vasil'ev (2001). About a detonation engine with external combustion. High-Speed Deflagration and Detonation: Fundamentals and Control.

[4] Korobeinikov V. P. et al. (1972). Propagation of Blast Waves in a Combustible Gas. Astronautica Acta, 17.

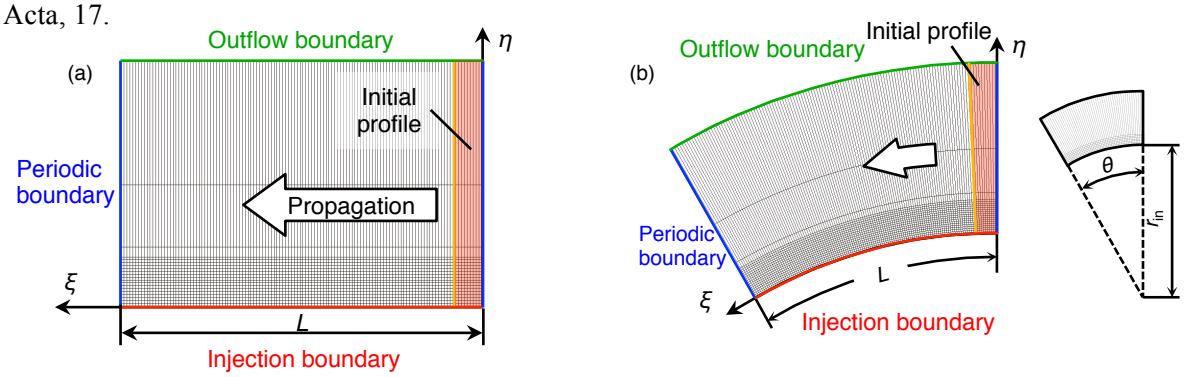

Figure 1. Computational domains of this study. (Every 20 points in each direction) (a): Rectangular flow field. (b): Arc-shaped flow field.

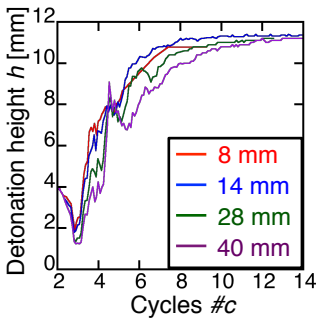

Figure 2. #c history of the detonation height as the height validation in the rectangular flow field in the case of L = 100 mm.

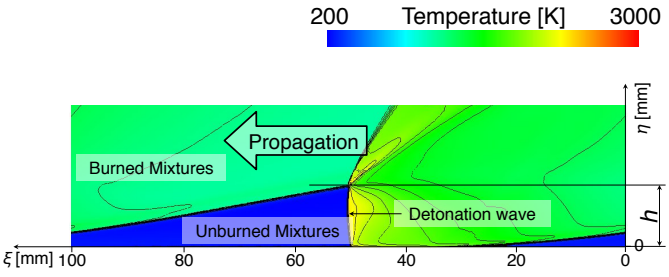

Figure 3. Steady flow field in L = 100 mm at #c = 8.50 in the rectangular flow field.

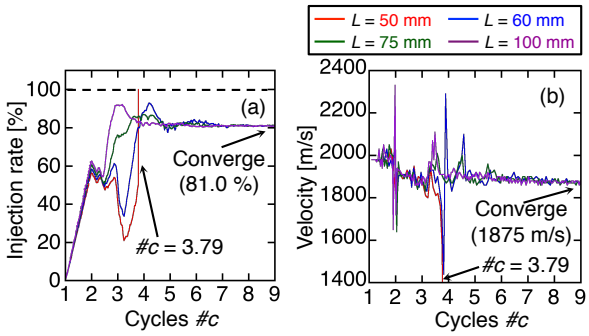

Figure 4. #c histories of the injection rate and the propagation velocity in the rectangular flow field. (a): The injection rate. (b): The propagation velocity.

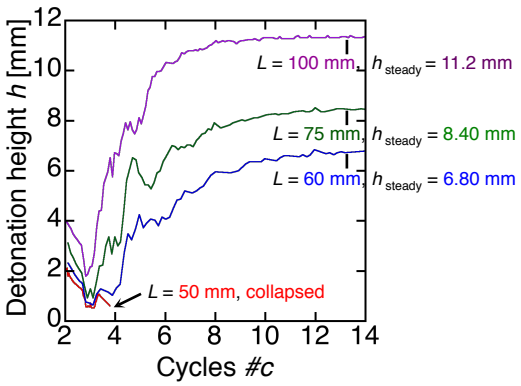

Figure 5. #c history of the detonation height in the rectangular flow field.

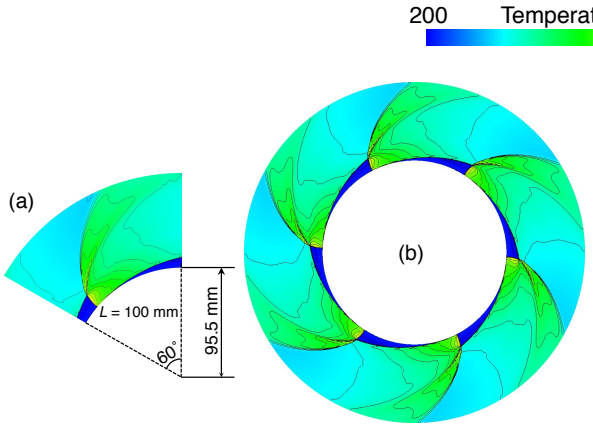

Figure 6. Steady flow field in r_{in} = 95.5 mm. There are 6 waves around the cylinder. (a): Initial state corresponding to #c = 9.83 in the arc-shaped flow field. (b): The state 200 μs after the restart.

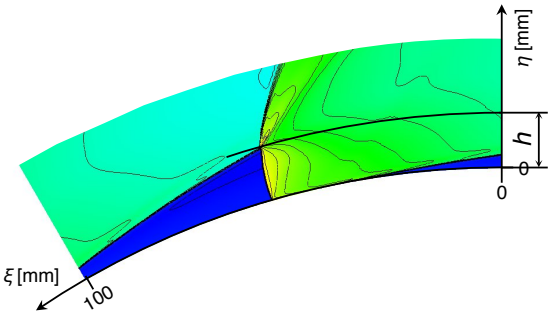

Figure 7. Steady flow field in r_{in} = 191 mm (θ = 30°) at #c = 8.50 in arc-shaped flow field in the case of L = 100 mm.

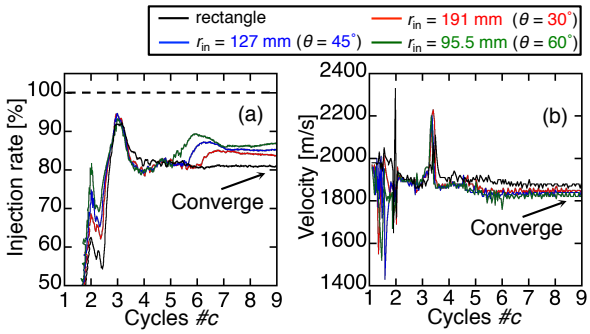

Figure 8. #c histories of the injection rate and the propagation velocity in stable cases of the arc-shaped flow field of L = 100 mm. (a): The injection rate. (b): The propagation velocity.

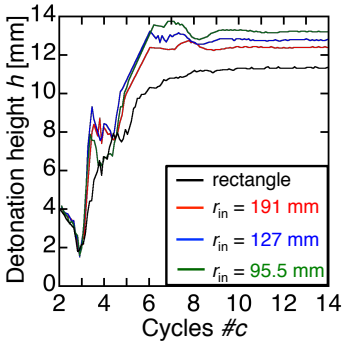

Figure 9. #c history of the detonation height in the arc-shaped flow field at constant L = 100 mm.

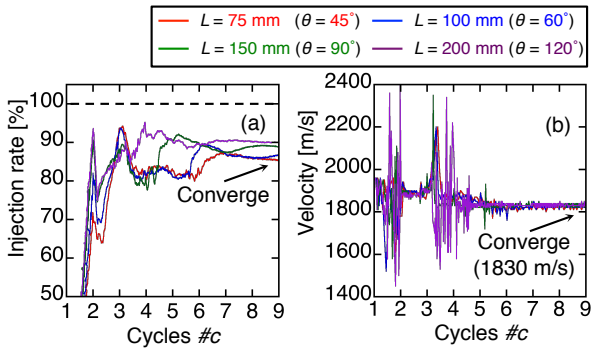

Figure 10. #c histories of the injection rate and the propagation velocity in stable cases of the arc-shaped flow field, r_{in} = 95.5 mm. (a): The injection rate. (b): The propagation velocity.

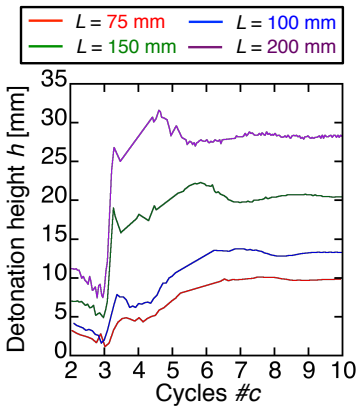

Figure 11. #c history of the detonation height in the arc-shaped flow field at constant r_{in} = 95.5 mm.

Table 1: The values of h_{steady} and D_{steady} in the rectangular flow field.

L [mm]	h_{steady} [mm]	h_{steady}/L	D_{steady} [m/s]
60	6.80	0.113	1875
75	8.40	0.112	1875
100	11.2	0.112	1875

Table 2: The values of h_{steady}, $h_{collapse}$ and D_{steady} in the arc-shaped flow field at constant L =100 mm. L_h is the length of inner wall at $r_{in} + h_{steady}$. D_h is the propagation velocity at the highest point of the detonation front. $D_{h/2}$ is derived from the average of D_{steady} and D_h.

r_{in} [mm]	θ [degree]	h_{steady} [mm]	$h_{collapse}$ [mm]	h_{steady}/L	L_h [mm]	h_{steady}/L_h	D_{steady} [m/s]	D_h [m/s]	$D_{h/2}$ [m/s]
rectangle ($r_{in} = \infty$, $\theta = 0°$)		11.2	-	0.112	-	-	1875	-	-
191	30	12.4	-	0.124	106	0.116	1850	1965	1908
127	45	12.8	-	0.128	110	0.117	1840	2019	1930
95.5	60	13.3	-	0.133	114	0.117	1830	2076	1953
79.6	72	-	14.2 (#c = 5.63)	-	118	-	-	-	-
63.7	90	-	13.8 (#c = 5.31)	-	122	-	-	-	-

Table 3: The values of h_{steady}, $h_{collapse}$ and D_{steady} in the arc-shaped flow field at constant r_{in} = 95.5 mm. L_h is the length of inner wall at $r_{in} + h_{steady}$. D_h is the propagation velocity at the highest point of the detonation front. $D_{h/2}$ is derived from the average of D_{steady} and D_h.

L [mm]	θ [degree]	h_{steady} [mm]	h_{steady}/L	L_h [mm]	h_{steady}/L_h	D_{steady} [m/s]	D_h [m/s]	$D_{h/2}$ [m/s]
75	45	9.84	0.131	82.7	0.119	1830	2005	1918
100	60	13.3	0.133	110	0.117	1830	2076	1953
150	90	20.5	0.137	182	0.113	1830	2222	2026
200	120	28.4	0.142	259	0.109	1830	2369	2100